Published in final edited form as:
J Surg Res. 2012 June 15; 175(2): 359–368. doi:10.1016/j.jss.2011.03.070.

Mechanical evaluation of decellularized porcine thoracic aorta

Yu Zou[1] and **Yanhang Zhang**[1,2]

[1]Department of Mechanical Engineering Boston University 110 Cummington Street, Boston, MA 02215

[2]Department of Biomedical Engineering Boston University 110 Cummington Street, Boston, MA 02215

Abstract

Background—Decellularized tissues are expected to have major cellular immunogenic components removed and in the mean time maintain similar mechanical strength and extracellular matrix (ECM) structure. However, the decellularization processes likely cause alterations of the ECM structure and thus influence the mechanical properties. In the present study, the effects of different decellularization protocols on the (passive) mechanical properties of the resulted porcine aortic ECM were evaluated.

Methods—Decellularization methods using anionic detergent (sodium dodecyl sulfate), enzymatic detergent (Trypsin), and non-ionic detergent (tert-octylphenylpolyoxyethylen (Triton X-100)) were adopted to obtain decellularized porcine aortic ECM. Histological studies and scanning electron microscopy were performed to confirm the removal of cells and to examine the structure of ECM. Biaxial tensile testing was used to characterize both the elastic and viscoelastic mechanical behaviors of decellularized ECM.

Results—All three decellularization protocols remove the cells effectively. The major ECM structure is preserved under SDS and Triton X-100 treatments. However, the structure of Trypsin treated ECM is severely disrupted. SDS and Triton X-100 decellularized ECM exhibits similar elastic properties as intact aorta tissues. Decellularized ECM shows less stress relaxation than intact aorta due to the removal of cells. Creep behavior is negligible for both decellularized ECM and intact aortas.

Conclusion—SDS and Triton X-100 decellularized ECM tissue appeared to maintain the critical mechanical and structural properties and might work as a potential material for further vascular tissue engineering.

Keywords

Decellularization; extracellular matrix; biaxial tensile testing; stress relaxation; creep; elastin; collagen; aorta

1. Introduction

The clinical need for the development of substitute vessels is quite obvious. For example, coronary and peripheral vascular bypass grafting is now performed more than 600,000 times annually in the United States and Europe to treat cardiovascular disease. During a bypass,

Corresponding author: Katherine Yanhang Zhang Clare Boothe Luce Assistant Professor Department of Mechanical Engineering Department of Biomedical Engineering Boston University 110 Cummington Street, Boston MA 02215 yanhang@bu.edu Phone: (617)358-4406 Fax: (617)353-5866.

the vascular surgeon creates a new pathway for blood flow using a natural or artificial substitute vessel. Autologous vessels are preferred as graft material; however, these vessels may not be an option for patients who have undergone previous bypass surgery or who do not have vessels of appropriate quality [1]. Tissue engineered materials have gained great attention in replacement of the malfunctioning or diseased cardiovascular tissues. The challenge of tissue engineering blood vessels lies in the requirement of both mechanical properties of native vessels and also the anti-thrombotics properties [2]. Since decellularization is considered to reduce the immunological response, decellularized tissues have become promising material in the field of tissue engineering for transplant and grafting. They have been successfully used in many pre-clinical studies [3–6] and even human clinical applications [7, 8]. Decellularization techniques have been applied to many types of tissues/organs, including heart valve [6, 9], bladder [10], ligament [11], tendon [12], vein [13] and artery [14, 15].

Decellularized tissues are expected to have all cellular and nuclear material efficiently removed while maintain similar composition, biological activity and mechanical integrity of the ECM [16]. The remaining ECM can be seeded with host's native cells *in vitro* before transplantation or *in vivo* after implantation [17]. Various decellularization protocols have been developed which may involve a combination of physical, chemical or enzymatic methods using different detergents or enzymatic agents to remove cells and cellular debris [16]. Among these decellularization protocols, the most commonly used methods include using anionic detergent sodium dodecyle sulfate (SDS) [18–20], enzymatic agent Trypsin [21, 22], and non-ionic detergent Triton X-100 (tert-octylphenylpolyoxyethylen) [23, 9].

Although decellularization techniques have been broadly applied to native tissues, there is still limited information on the matrix structure and mechanical properties after the decellularization process. It is noted that changes in the ECM structure after decellularization process would affect the mechanical properties of the tissue [16]. Previous studies investigated the matrix structure of decellularized tissue using combined histology and microscopy techniques [24–27]. Several mechanical studies were performed to understand the mechanical integrity of decellularized arteries [4, 14, 15], and decellularized aortic valve leaflet [28]. However, little was found on the time-dependent mechanics of decellularized tissues. Successful decellularization will produce an ECM that possesses anisotropic hyperelasticity, as usually seen in the intact aortas [29]. In the a few previous mechanical studies on decellularized arteries [4, 14, 15], loading has been limited to uniaxial stretching, which ignores the multiaxial loading state under physiological conditions, and thus the intrinsic anisotropic properties of soft tissue. Planar biaxial tensile test with independent control of load in both perpendicular directions has been used broadly to study the mechanical behavior of various soft biological tissues [29, 30–34]. Although it cannot fully replicate the physiological loading conditions, biaxial tensile test is sufficient on elucidating the anisotropic mechanical properties of soft tissues with plane stress assumptions. Such capabilities make it a useful tool for in vitro understanding of tissue mechanics.

The objective of the present study is to evaluate three commonly used decellularization protocols with an emphasis on understanding the relationships between structural changes and mechanical alteration. Three decellularization protocols were adopted to obtain the decellularized porcine aortic ECM. SDS was chosen as an anionic detergent, Trypsin as an enzymatic agent, and Triton X-100 as a non-ionic detergent. Scanning electron microscopy (SEM) and histology studies were used to confirm the removal of cells and to investigate the composition and structure of tissue samples. Planar biaxial tensile, biaxial stress relaxation and creep tests were performed to study the mechanical behavior of decellularized ECM.

Results from this study provide insight into the effects of structural changes on the elastic and viscoelastic properties of arteries after decellularization.

2. Materials and Methods

2.1 Sample preparation

Fresh porcine descending thoracic aortas were harvested from a local slaughter house and transported on ice to lab. Immediately after arrival, the aortas were cleaned off adherent tissues and fat, dissected, and rinsed in DI water. Square samples of about 2cm×2cm were cut from the middle section of the aortas to minimize the changes of the mechanical properties along the longitudinal position of aorta [33]. The decellularization process of aortic tissue samples was performed according to the protocols described later. Mechanical testing was performed immediately after the completion of decellularization to minimize the possible degradation effect of the microstructural components in the ECM. Three decellularization protocols were adopted to obtain the decellularzied extracellular matrix (ECM) of porcine thoracic aorta, described as follows:

The first decellularization protocol was based on SDS treatment [18, 19]. Porcine aorta samples were incubated in hypotonic 10mM Tris buffer (pH=8.0) with 0.1% EDTA for 1 hour, and then subjected to continuous shaking at room temperature in a solution of 0.1% sodium dodecyle sulfate (SDS) (MP Biomedicals LLC) with Tris buffer (10mM Tris, pH8.0), together with RNase A (20μg/ml) and DNase (0.2mg/ml) for 48 hrs.

An enzymatic agent, Trypsin, was used as another method for decellularization [21, 22]. Briefly, tissue samples were incubated in 0.5% Trypsin and 0.2% EDTA in hypotonic Tris buffer (10mM Tris, pH8.0), also with RNase A (20μg/ml) and DNase (0.2mg/ml) at 37°C for 48 hrs.

The third method is based on the Triton X-100 (tert-octylphenylpolyoxyethylen) decellularization process [9]. Aorta samples were treated with continuous shaking in a solution of 1% Triton X-100 (Bio-Rad) with 0.2% EDTA in 10mM Tris buffer with 20μg/ml RNase A and 0.2mg/ml DNase at 37°C for 48 hrs.

After the decellularization process, the tissue samples were carefully washed several times in 1× PBS to remove the chemical residues. Dimensions of aortic samples were measured and recorded before and after the decellularization process. A digital caliper was used to measure the length, width, and thickness of each sample. An average of six measurements was recorded and used in the mechanical calculations. The decellularized ECM samples were kept in 1× PBS for further testing. All the chemicals used in this study were purchased from Fisher Scientific unless otherwise specified.

2.2 Scanning electron microscopy

Tissue samples of 5mm long strips were dissected from the decellularized and intact aortas. Samples were fixed in Karnovsky's fixative kit (2% paraformaldehyde, 2.5% glutaraldehyde and 0.1M sodium phosphate buffer) for 1 h and then dehydrated in a series of graded ethanol. The samples were then dried using a Denton vacuum DCP-1 CO_2 critical point dryer. A very thin layer of platinum (20 nm) was coated on the cross section of the samples using a Sputter Coater (Cressington 108). SEM was performed at 5 kv on the cross sections of the tissue samples using a JOEL JSM-6100 SEM machine.

2.3 Histological studies

Histological images were taken to validate the removal of smooth muscle cells (SMCs) in the decellularized ECM. Tissue samples were fixed in 10% formalin buffer and then

embedded in paraffin. Sections of about 6μm in thickness were cut and stained. Hematoxylin and Eosin (H&E) and Movat's pentachrome stain stains were performed to examine the presence of cells, elastin and collagen.

2.4 Planar biaxial tensile testing

Mechanical testing was performed using a planar biaxial tensile testing device, which has been used in our previous studies on the mechanical characterization of the elastic and viscoelastic behaviors of aortic elastin [29, 33]. Briefly, a roughly square-shaped specimen is mounted so that it can be stretched along both in-plane directions. Four marker dots forming a 5mm × 5mm square are placed in the center of the testing specimen, and a CCD camera is used to trace the position of the marker dots and determine the tissue strains in both directions throughout the deformation. The load applied to the specimen, i.e., tensile tension, is measured by the load cell. Decellularized ECM samples were tested under equi-biaxial tensile tests, and biaxial stress relaxation and creep tests to study to elastic and viscoelastic mechanical properties, respectively. Corresponding intact aorta samples were also tested for comparison.

All tests were performed in 1× PBS solution at room temperature following the test protocols described in our previous studies [29, 33]. An initial 3g tare load was applied before biaxial tensile testing to obtain flatness and tautness of the soft tissue. Tissue samples were first preconditioned for 8 cycles with 15s of half cycle time equi-biaxially to obtain repeatable material response. For biaxial tensile test, a membrane tension was applied to the samples starting from the initial tare load for 8 cycles with 15s of half cycle time. The peak membrane tension varied from 150N/m to 180N/m. The force-stretch response in both the longitudinal and circumferential directions was recorded. Cauchy stresses vs. Green-Lagrange strain were used to describe the anisotropic hyperelastic behavior of aorta and decellularized ECM. The Cauchy stresses in the in the longitudinal (x_1) and circumferential (x_2) directions of the tissue sample were obtained by [33]:

$$\sigma_1=\frac{F_1\lambda_1}{hL_{02}},\quad \sigma_2=\frac{F_2\lambda_2}{hL_{01}} \tag{1}$$

where σ_i(i = 1, 2) is the Cauchy stress, F_i and λ_i (i = 1, 2) are the load and stretch in the x_i (i = 1, 2) direction; h and L_{0i} (i = 1, 2) represent the thickness and length of the sample, respectively, before it was stretched. The Green-Lagrange strain can be calculated by [35]:

$$E_1=\frac{1}{2}\left(\lambda_1^2-1\right),\quad E_2=\frac{1}{2}\left(\lambda_2^2-1\right) \tag{2}$$

where E_i (i = 1, 2) is the Green-Lagrange strain in the x_i direction.

For stress relaxation test, an equibiaxial tensile test was first applied to the sample. Immediately after the 8th cycle of the test, the sample was quickly stretched to the target stretch with a rise time of 2 s and held at this constant stretch for 1800 s. Similarly, for creep test, the tissue sample was quickly loaded within 2 s and then the tension was kept constant for 1800 s. The tension or stretch in both the longitudinal and circumferential directions was recorded with during the entire testing period for stress relaxation or creep tests, respectively.

To be noted, stress relaxation preconditioning was validated to be essential to achieve a repeatable stress relaxation behavior in soft tissues in our previous study [29]. To obtain repeatable viscoelastic responses of the decellularized ECM, five cycles of stress relaxation tests were performed and the data from the fifth cycle was used in the present study.

Samples were allowed to equilibrate in free floating state in the solution bath for 30min between stress relaxation and creep tests. Additionally, the initial stress level was also observed to be an important factor which will influence the rate of stress relaxation of both aorta and decellularized ECM samples. In this work, the initial stress level was kept in the range of 130 to 150 kPa to reduce the effect of initial stress levels, which also has close physiological relevance [36, 37].

2.5 Statistical analysis

Averaged results are expressed as mean ± standard error of the mean. Sstatistical analysis was performed using one-way analysis of variance (ANOVA) and two-tail two-sample t-test assuming unequal variances. Differences are considered statistically significant when $p < 0.05$.

3. Results

SEM was performed on the cross section along the circumferential direction of the intact and decellularized aortas to examine the morphology and structure. As shown in Figure 1, in the intact artery, a dense structure is present with smooth muscle cells (SMCs) embedded in the cross-linked ECM network of elastin and collagen fibers (Fig.1a). After the SDS and Triton X-100 decellularization treatment, the ECM network of fibers is better revealed with the removal of SMCs. Images in Figs. 1b and 1c show detailed porous structures of the crosslinked network. After decellularization with 0.5% Trypsin, although SMCs are successfully removed, the ECM structure is severely disrupted (Fig. 1d). The fibers are sparsely distributed demonstrating breakage of crosslinks and fibers within the ECM.

Histological study further validates the removal of SMCs after decellularization (Fig. 2). Intact aorta shows characteristic organization of SMCs and ECM in both Movat's pentachrome stain and H&E stain (Figs. 2a, e). H&E stain images confirm the complete removal of cells for all three decellularization protocols (Figs. 2f, g, h). Movat's pentachrome stain shows a cross-linked network of collagen and elastin fibers in the SDS and Triton X-100 treated ECM (Figs. 2b, c). However, the network structure of the Trypsin decellularized ECM is disrupted leaving only scattered fibers (Figs. 2d, h).

Both SEM and histology results reveal that Trypsin decellularization protocol severely destroys the structure of ECM. After 48 hrs, Trypsin treated sample becomes a semi-transparent viscous gel-like structure. Figure 3 shows an optical image of the Trypsin treated ECM under equi-biaxial tension of 20N/m. The remaining scattered fibers within the sample can be seen under light microscope and tend to align in the loading directions. Upon loading, the sample failed to stay in shape which is characterized by a skewed distribution of the four marker dots, as shown in Fig. 3. Our results show that the Trypsin treatment causes extensive degeneration and fragmentation of the ECM and fails to achieve a structurally preserved decellularized ECM. Therefore, only the mechanical behaviors of SDS and Triton X-100 treated ECM were evaluated in this study.

The dimensions of the tissue samples were measured before and after decellularization. Figure 4 shows the normalized size change, which is calculated by normalizing the sample dimensions after decellularization by the original dimensions of the corresponding intact aorta, for ECM samples treated with SDS (n = 9) and Triton X-100 (n = 9). For both decellularization treatments, the side lengths of the ECM samples decrease less than 1% compared to the intact aorta, which can be considered negligible. However, the thickness decreases significantly to 79.4% ± 5.71% ($p = 0.0000016$) and 79.8% ± 5.81% ($p = 0.00027$) of the intact aorta after SDS and Triton X-100 treatments, respectively. There are no significant differences between the size changes from the two protocols ($p = 0.454$). The

dimensions of Trypsin treated ECM were not measured since these swelled gel-like samples could hardly stay in shape.

In order to assess the effects of decellularization on the elastic behavior, equi-biaxial tensile tests were performed on the aorta tissue samples before and after decellularization (SDS n = 9, Triton X-100 n = 9). Representative comparison curves of the Cauchy stress vs. Green-Lagrange strain responses from decellularized ECM and corresponding intact aorta samples are shown in Figure 5. The decellularized ECM shows similar elastic responses as the intact aorta. It exhibit almost linear elasticity initially with elastin being the major load bearing element. Strain stiffening happens when the load continues to increase due to the involvement of collagen. Decellularized ECM also possesses similar anisotropic hyperelastic behavior as aorta with the circumferential direction being stiffer than the longitudinal direction. To better elucidate the changes of stiffness and compare the mechanical behavior of decellularized and intact aorta, tangent modulus in the longitudinal and circumferential directions was calculated for each tissue sample by differentiating the stress-strain curves under equi-biaxial plane stress assumptions, i.e., $E_t \approx 1/2\ d\sigma/d\varepsilon$ [38], and then averaged. As shown in Fig. 6, in the longitudinal direction, the tangent modulus decreases at a maximum of 13.5% for the SDS decellularized samples, and 13.1% for Triton X-100 treated ones, but the changes are statistically insignificant ($p > 0.05$). In the circumferential direction, the SDS decellularized ECM has very similar tangent modulus as the intact arteries, especially at lower strains (less than 0.1) (Fig. 6a). The Triton X-100 decellularized ECM has almost identical elastic tangent modulus in the circumferential direction as the corresponding intact arteries (Fig. 6b).

Figure 7(a) shows the representative stress relaxation curves of decellularized ECM and intact aorta. All tissue samples were tested at the initial stresses of 143.96 ± 8.89 kPa to eliminate the effect of initial stress levels on the rate of stress relaxation [29]. The stresses were normalized to that at the beginning of the holding period. Results show that aorta exhibited significantly more stress relaxation than decellularized ECM in both the circumferential and longitudinal directions. Moreover, most of the stress relaxation happens during the first 10 min of the holding period. The maximum stress relaxation was obtained by normalizing the total stress drop to the stress at the beginning of the holding period. Figure 7(b) shows the maximum stress relaxation for SDS (n=5) and Triton X-100 treated ECM (n=4), and intact aorta (n=4). The SDS and Triton X-100 decellularized ECM relax stresses to 85.49% ± 1.51% and 85.10% ± 1.58% of the initial stresses, respectively. Intact porcine aorta exhibits stress relaxation to 79.79% ± 3.03% of initial stresses. Aorta relaxes significantly more than the decellularized ECM ($p = 0.000013$), however the differences between SDS and Triton X-100 treated ECM samples are negligible ($p = 0.855$).

Creep tests show that creep responses are negligible for all tissue samples, as shown in Figure 8. The maximum normalized creep of SDS (n=4) and Triton X-100 (n=4) decellularized ECM, and intact aorta (n=3) is 1.77 ± 1.11%, 1.67 ± 0.54%, and 1.68 ± 1.25%, respectively. There are no significant differences between all the tissue samples ($p = 0.949$).

Discussion

The present study examined the efficiency of SDS, Trypsin, and Triton X-100 decellularization protocols on porcine thoracic aortas with an emphasis on understanding the relationships between structural changes and mechanical alteration. The Trypsin decellularization protocol effectively removes all the cells and nuclear components; however, substantial disruption of the ECM is accompanied with this technique. Similar to our findings, a number of previous studies have reported the extensive destruction of the

matrix structure caused by Trypsin-based protocols. Meyer et al. [6] compared different decellularization techniques of rat aortic valve and observed severe destruction of the ECM from histological study and loss of noncollagen elements indicated by collagen assays after Trypsin decellularization. They suggested that Trypsin treatment destroy the small soluble and nonfibrillar proteins, proteoglycans and glycosaminoglycans (GAGs). Grauss et al. [17] also reported an almost complete loss of elastin, GAGs, a disruption of collagen, and a decrease in fibronectin of the aortic valves with Trypsin treatment. These structural damages will impact the durability and mechanical properties of the tissue. Our results further demonstrate the Trypsin decellularized aortic ECM become a loose structure of limited fibers and is unable to sustain mechanical tension.

Decellularization using SDS and Triton X-100 treatments are effective at removing cellular elements while maintaining the major structure of the elastin and collagen network in the ECM (Fig.1 & Fig.2). Although Grauss et al. [17] found that 1% Triton X-100 were ineffective in reducing cellular components of rat aortic valve, most other researchers found it adequate and effective. Bader et al. [9] performed 1% Triton X-100 decellularization of porcine valves and found that the procedure resulted in an almost complete removal of the origincal cells with a loosened three dimensional matrix at interfibrillar zones. Similar results were observed by Kasimir et al. [27] and Liao et al. [39]. Liao et al. [39] also observed an increase in pore size of tissues treated with Triton X-100 compared with tissues treated with SDS. Meyer et al. [6] lowered the concentration of Triton X-100 solution to 0.5% and still achieved very effective decellularization. SDS decellularization is considered to be the mildest treatment to preserve the major structural components of elastin and collagen in previous aortic valve studies [17, 39]. However, earlier study using SDS treatment was reported to destabilize the collagen triple helical domain and to swell the elastin network [40]. This controversial finding may due to the differences in incubation time and SDS concentration used in the decellularization process, and might also come from the specific characterization of diverse tissue specimens. Both Grauss et al. [17] and Liao et al. [39] used 0.1% SDS on aortic valves for 24 and 48 hours respectively; while Samouillan et al. [40] treated aortic roots in 1% SDS for 64 hours total.

The decellularized ECM remains to be a very anisotropic hyperelastic material with the circumferential direction being much stiffer than the longitudinal direction (Fig. 5). Overall, the hyperelastic mechanics integrity is maintained in the SDS and Triton X-100 decellularized ECM. Dellularized ECM exhibits similar stress strain responses as the intact aortic tissues. While the small changes in the tangent modulus may reflect minor structural alterations of the matrix structure, these changes are not statistically significant. Several previous studies have reported changes in the mechanical properties of decellularized ECM, however discrepancies exist. Here we briefly compare the previous findings with our results and explain the possible sources of discrepancy. Increased extensibility in the decellularized porcine aortic valves was reported using SDS, Triton X-100 and Trypsin protocols [39]. The change was explained by the increased ability for the circumferentially oriented collagen fibers to rotate in the decellularized tissue matrix. In this study, the extensibility was determined by areal strain under 60N/m tension for each sample. However, with the significant decrease in thickness after the decellularization process, it may raise doubts in the comparison of extensibility of samples with different thicknesses under the same tension level. Williams et al. [14] determined the mechanical properties of native and decellularized rabbit carotid arteries using uniaxial tests and found an increase of tensile modulus after decellularization. They also reported a decrease of extensibility of the decellularized arteries. Such changes were explained by the loosening and uncrimping of collagen fiber network in the decellularized samples [14]. A more recent work from Fitzpatrick et al. [15] investigated the mechanical behavior of decellularized porcine aorta using uniaxial tensile tests as well. They used three decellularization protocols, Triton X-100, SDS, and a combination of Triton

X-100 and sodium-deoxycholate. Their results showed a decreased stiffness in all the decellularized samples with different decellularization protocols. The difference in mechanical testing method may be another possible reason for the different findings of the mechanical behavior of decellularized tissues, since uniaxial tensile testing cannot fully characterize the anisotropic mechanical responses of soft tissues and may induce fiber reorientation under uniaxial loading [41].

There is very limited information on the time-dependent mechanics of decellularized tissues. Decellularized ECM shows less stress relaxation compared to native aorta (Figure 7), as expected, due to the loss of smooth muscle cells which can cause a more significant stress relaxation than collagen or elastin. Williams et al. [14] claimed that there was no significant difference of stress relaxation between native and decellularized arteries. However, in their study, native arteries were stored at −20°C before decellularization, which would damage the activity of smooth muscle cells. Moreover, the initial stress level is another crucial factor to influence the rate of stress relaxation of soft tissues. Our recent study [29] showed that the rate of stress relaxation increases linearly with the initial stress level for both intact and decellularized aorta. Consequently, in the present study all samples were tested at the initial stresses of 143.96 ± 8.89 kPa to eliminate the influence of initial stress levels on stress relaxation behavior. Creep behavior was negligible for all decellularized and native aortas (Figure 8). This unique behavior of very little creep compared with obvious stress relaxation was observed before for soft biological tissues [29, 39, 41, 42], and was attributed to different mechanisms of stress relaxation and creep behavior. However the mechanisms are not fully understood. Future microstructural studies are needed to better understand the effect of mechanical loading on viscoelasticity.

Conclusions

In the present study, the elastic and viscoelastic behaviors of decellularized aortic ECM were examined using planar biaxial tensile testing. Three commonly used decellularization protocols were evaluated in porcine thoracic aortas for efficiency of cell removal and ability to maintain mechanical integrity. Changes in mechanical function were related to the structure of the decellularized ECM. SEM and histology studies show that the cells were removed completely in all three decellularization protocols. However, the ECM structure was severely disrupted in the Trypsin treated samples which causes the loss of mechanical functionality. SDS and Triton X-100 treatments preserved the major structure and function of ECM and are considered an effective approach to decellularize aortic tissue. ECM from these two decellularization proctocals exhibited similar elastic properties as intact aortas under biaxial tensile testing. Less stress relaxation was observed as expected due to the removal of SMCs. No obvious creep behavior was found in both decellularized and native aorta samples. In conclusion, SDS and Triton X-100 decellularized ECM tissue appeared to maintain the critical mechanical and structural properties and might work as a potential material for further vascular tissue engineering.

Acknowledgments

We would like to acknowledge the financial support from the National Institutes of Health (HL098028) and the CAREER award from the National Science Foundation (CMMI-1038208).

References

1. Salacinski HJ, Goldner S, Giudiceandrea A, Hamilton G, Seifalian AM. The mechanical behavior of vascular grafts: a review. Journal of Biomaterials Application. 2001; 15:241–278.
2. Ratcliffe A. Tissue engineering of vascular grafts. Matrix Biology. 2000; 19:3553–357.

3. Conklin BS, Richter ER, Kreutziger KL, Zhong D-S, Chen C. Development and evaluation of a novel decellularized vascular xenograft. Medical Engineering & Physics. 2002; 24:173–183. [PubMed: 12062176]
4. Dahl SLM, Koh J, Prabhakar V, Niklason LE. Decellularized native and engineered arterial scaffolds for transplantation. Cell Transplantation. 2003; 12:659–666. [PubMed: 14579934]
5. Amiel GE, Komura M, Shapira O, Yoo JJ, Yazdani S, Berry J, Kaushal S, Bischoff J, Atala A, Soker S. Engineering of blood vessels from acellular collagen matrices coated with human endothelial cells. Tissue Engineering. 2006; 12:2355–2365. [PubMed: 16968175]
6. Meyer SR, Chiu B, Churchill TA, Zhu L, Lakey JRT, Ross DB. Comparison of aortic valve allograft decellularization techniques in the rat. Journal of Biomedical Materials Research Part A. 2006; 79:254–262. [PubMed: 16817222]
7. Metcalf MH, Savoie FH, Kellum B. Surgical technique for xenograft (SIS) augmentation of rotator-cuff repairs. Operative Techniques in Orthopaedics. 2002; 12:204–208.
8. Kolker AR, Brown DJ, Redstone JS, Scarpinato VM, Wallack MK. Multilayer reconstruction of abdominal wall defects with acellular dermal allograft (AlloDerm) and component separation. Annals of Plastic Surgery. 2005; 55:36–41. discussion 41–42. [PubMed: 15985789]
9. Bader A, Schilling T, Teebken OE, Brandes G, Herden T, Steinhoff G, Haverich A. Tissue engineering of heart valves-human endothelial cell seeding of detergent acellularized porcine valves. European Journal of Cardio-thoracic Surgery. 1998; 14:279–284. [PubMed: 9761438]
10. Atala A, Bauer SB, Soker S, Yoo JJ, Retik AB. Tissue-engineered autologous bladders for patients needing cystoplasty. The Lancet. 2006; 367:1241–1246.
11. Ingram JH, Korossis S, Howling G, Fisher J, Ingham E. The use of ultrasonication to aid recellularization of acellular natural tissue scaffolds for use in anterior cruciate ligament reconstruction. Tissue Engineering. 2007; 13:1561–1572. [PubMed: 17518726]
12. Nyland J, Larsen N, Burden R, Chang H, Caborn DN. Biochemical and tissue handling property comparison of decellularized and cryopreserved tibialis anterior tendons following extreme incubation and rehydration. Knee Surgery, Sports Traumatology, Arthroscopy: Official Journal of the ESSKA. 2009; 17:83–91.
13. Schaner PJ, Martin ND, Tulenko TN, Shapiro IM, Tarola NA, Leichter RF, Carabasi RA, DiMuzio PJ. Decellularized vein as a potential scaffold for vascular tissue engineering. Journal of Vascular Surgery. 2004; 40:146–153. [PubMed: 15218475]
14. Williams C, Liao J, Joyce EM, Wang B, Leach JB, Sacks MS, Wong JY. Altered structural and mechanical properties in decellularized rabbit carotid arteries. Acta Biomaterialia. 2009; 5:993–1005. [PubMed: 19135421]
15. Fitzpatrick JC, Clark PM, Capaldi FM. Effect of decellularization protocol on the mechanical behavior of porcine descending aorta. International Journals of Biomaterials. 2010 doi: 10.1155/2010/620503.
16. Gilbert TW, Sellaro TL, Badylak SF. Decellularization of tissues and organs. Biomaterials. 2006; 27:3675–3683. [PubMed: 16519932]
17. Grauss RW, Hazekamp MG, van Vliet S, Gittenberger-de Groot AC, DeRuiter MC. Decellularization of rat aortic valve allografts reduces leaflet destruction and extracellular matrix remodeling. The Journal of Thoracic and Cardiovascular Surgery. 2003; 126:2003–2010. [PubMed: 14688719]
18. Allaire E, Guettier C, Bruneval P, Plissonnier D, Michel J. Cell-free Arterial Grafts: Morphologic Characteristics of Aortic Isografts, Allografts, and Xenografts in Rats. Journal of Vascular Surgery. 1994; 19:446–456. [PubMed: 8126857]
19. Booth C, Korossis SA, Wilcox HE, Watterson KG, Kearney JN, Fisher J, Ingham E. Tissue Engineering of Cardiac Valve Prostheses I: Development and Histological Characterization of an Acellular Porcine Scaffold. Journal of Heart Valve Disease. 2002; 11:457–462. [PubMed: 12150290]
20. Korossis SA, Booth C, Wilcox HE, Watterson KG, Kearney JN, Fisher J, Ingham E. Tissue engineering of cardiac valve prostheses II: biomechanical characterization of decellularized porcine aortic heart valves. The Journal of Heart Valve Disease. 2002; 11:463–471. [PubMed: 12150291]

21. Steinhoff G, Stock U, Karim N, Mertsching H, Timke A, Meliss RR, Pethig K, Haverich A, Bader A. Tissue Engineering of Pulmonary Heart Valves on Allogenic Acellular Matrix Conduits: In Vivo Restoration of Valve Tissue. Circulation. 2000; 102:III50–III55. [PubMed: 11082362]
22. Cebotari S, Mertsching H, Kallenbach K, Kostin S, Repin O, Batrinac A, Kleczka C, Ciubotaru A, Haverich A. Constructionof autologous human heart valves based on an acellular allograft matrix. Circulation. 2002; 106:I63–I68. [PubMed: 12354711]
23. Wilson GJ, Courtman DW, Klement P, Lee JM, Yeger H. Acellular matrix: a biomaterials approach for coronary artery bypass and heart valve replacement. The Annals of Thoracic Surgery. 1995; 60:S535–S358.
24. Rieder E, Kasimir MT, Silberhumer G, Seebacher G, Wolner E, Simon P, Weigel G. Decellularization protocols of porcine heart valves differ importantly in efficiency of cell removal and susceptibility of the matrix to recellularization with human vascular cells. Surgery for Acquired Cardiovascular Disease. 2004; 127:399–405.
25. Elkins RC, Dawson PE, Goldstein S, Walsh SP, Black KS. Decellularized human valve allografts. The Annals of Thoracic Surgery. 2001; 71:S428–S432. [PubMed: 11388241]
26. Schmidt CE, Baier JM. Acellular vascular tissues: natural biomaterials for tissue repair and tissue engineering. Biomaterials. 2000; 21:2215–2231. [PubMed: 11026628]
27. Kasimir M-T, Rieder E, Seebacher G, Silberhumer G, Wolner E, Weigel G, Simon P. Comparison of different decellularization procedures of porcine heart valves. The International Journal of Artificial Organs. 2003; 26:421–427. [PubMed: 12828309]
28. Liao J, Joyce EM, Sacks MS. Effects of decellularization on the mechanical and structural properties of the porcine aortic valve leaflet. Biomaterials. 2008; 29:1065–1074. [PubMed: 18096223]
29. Zou Y, Zhang Y. The orthotropic viscoelastic behavior of aortic elastin network. Biomechanics and Modeling in Mechanobiology. 2010 Epub ahead of print.
30. Sacks MS, Sun W. Multiaxial mechanical behavior of biological materials. Annual Review of Biomedical Engineering. 2003; 5:251–284.
31. Geest JPV, Sacks MS, Vorp DA. The effects of aneurysm on the biaxial mechanical behavior of human abdominal aorta. Journal of Biomechanics. 2006; 39:1324–1334. [PubMed: 15885699]
32. Knezevic V, Sim AJ, Borg TK, Holmes JW. Isotonic biaxial loading of fibroblast-populated collagen gels: a versatile, low-cost system for the study of mechanobiology. Biomechanics and Modeling in Mechanobiology. 2002; 1:59–67. [PubMed: 14586707]
33. Zou Y, Zhang Y. An experimental and theoretical study on the anisotropy of elastin network. Annals of Biomedical Engineering. 2009; 37:1572–1583. [PubMed: 19484387]
34. Jhun CS, Evans MC, Barocas VH, Tranquillo RT. Planar biaxial mechanical behavior of bioartificial tissues possessing prescribed fiber alignment. Journal of Biomechanical Engineering. 2009; 131:081006. [PubMed: 19604018]
35. Humphrey, JD. Cardiovascular solid mechanics: cells, tissues, and organs. Springer-Verlag; New York: 2002.
36. Guo X, Kassab GS. Distribution of stress and strain along the porcine aorta and coronary arterial tree. Am J Physiol Heart Circ Physiol. 2004; 286:H2361–H2368. [PubMed: 15148060]
37. Stergiopulos N, Vulliemoz S, Rachev A, Meister J-J, Greenwald SE. Assessing the homogeneity of the elastic properties and composition of the pig aortic media. Journal of Vascular Research. 2001; 38:237–246. [PubMed: 11399896]
38. Zhang Y, Dunn ML, Drexler ES, McCowan CN, Slifka AJ, Ivy DD, Shandas R. A microstructural hyperelastic model of pulmonary arteries under normo- and hypertensive conditions. Annals of biomedical engineering. 2005; 33:1042–1052. [PubMed: 16133913]
39. Liao J, Yang L, Grashow J, Sacks MS. The relationship between collagen fibril kinematics and mechanical properties in the mitral valve anterior leaflet. Journal of Biomechanical Engineering. 2007; 129:78–87. [PubMed: 17227101]
40. Samouillan V, Dandurand-Lods J, Lamure A, Maurel E, Lacabanne C, Gerosa G, Venturini A, Casarotto D, Gherardini L, Spina M. Thermal analysis characterization of aortic tissues for cardiac valve bioprostheses. Journal of Biomedical Materials Research. 1999; 46:531–538. [PubMed: 10398014]

41. Stella JA, Liao J, Sacks MS. Time-dependent biaxial mechanical behavior of the aortic heart valve leaflet. Journal of Biomechanics. 2007; 40:3169–3177. [PubMed: 17570376]

42. Grashow JS, Sacks MS, Liao J, Yoganathan AP. Planar biaxial creep and stress relaxation of the mitral valve anterior leaflet. Annals of Biomedical Engineering. 2006; 34:1509–1518. [PubMed: 17016761]

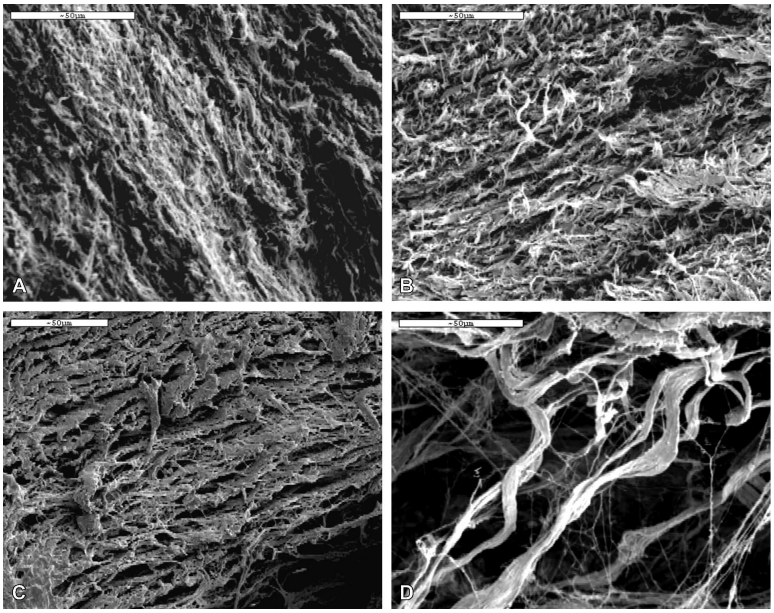

Figure 1.
SEM images of the cross section in the circumferential direction of (a) native porcine aorta, (b) SDS decellularized ECM, (c) Triton X-100 decellularized ECM, and (d) Trypsin decellularized ECM. All scale bars represent 50 μm.

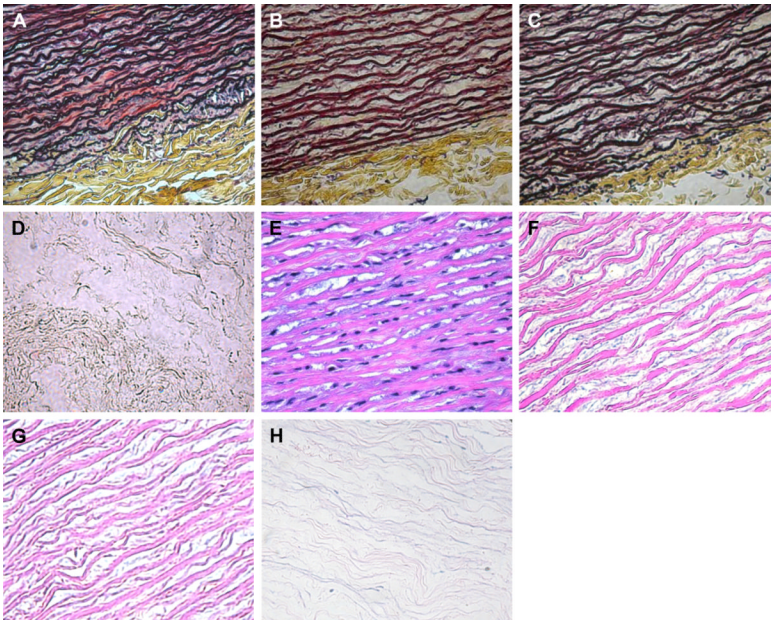

Figure 2.
Histology images of the cross section in the circumferential direction of (a, e) native porcine aorta, (b, f) SDS decellularized ECM, (c, g) Triton X-100 decellularized ECM, and (d, h) Trypsin decellularized ECM. Movat's pentachrome stains elastin purple-black, collagen yellow, and cells red (a–d). Hematoxylin and Eosin (H&E) stains elastin and collagen pink, and cells purple-blue (e–h).

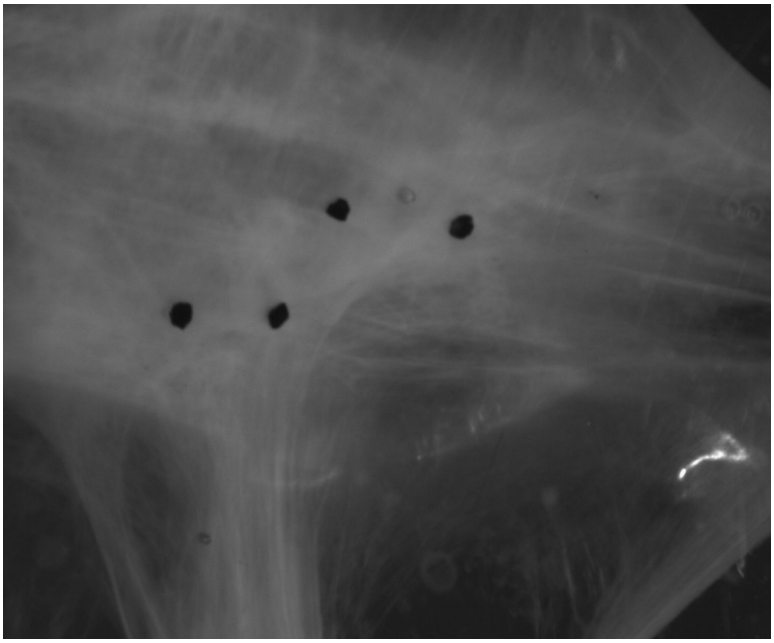

Figure 3.
Image of Trypsin decellularized ECM under equi-biaxial tensile test with 20N/m membrane tension. Loss of mechanical integrity was manifested by the presence of scattered fibers and skewed distribution of the four strain tracing marker dots.

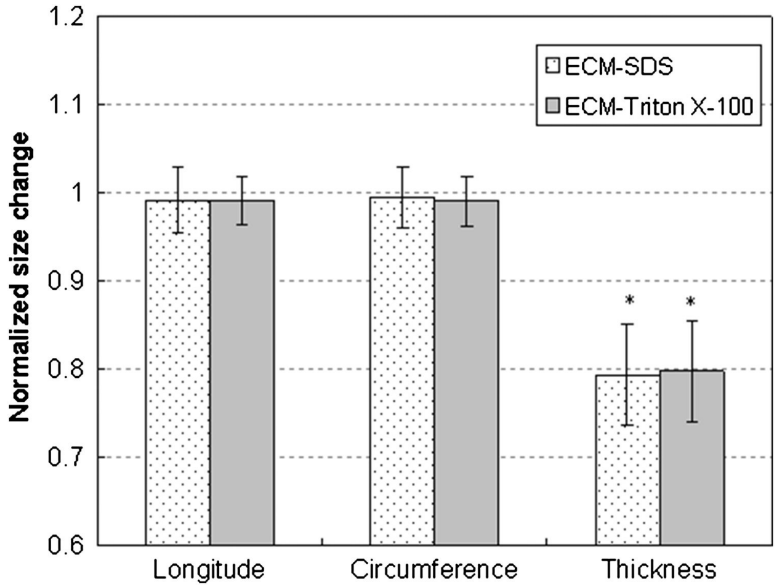

Figure 4.

Normalized size change of the aortic ECM after the SDS and Triton X-100 decellularization processes. Normalized sizes of ECM were obtained by dividing the sizes of ECM samples by the sizes of the corresponding aorta samples. * indicates the difference is statistically significant ($p < 0.05$).

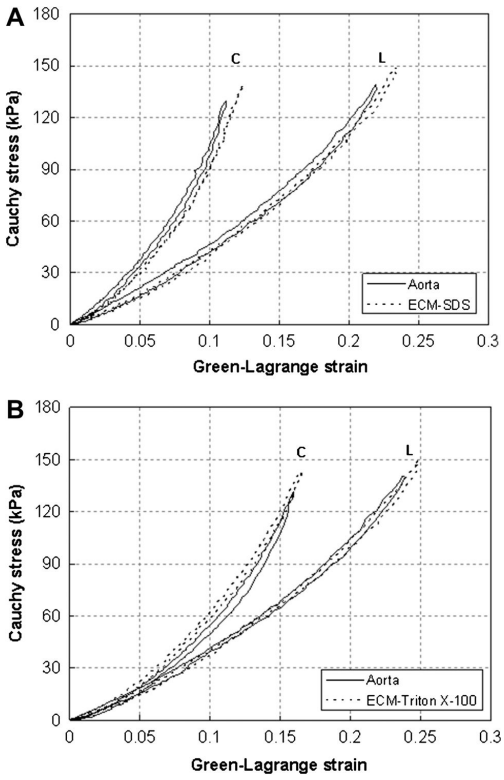

Figure 5.
Representative Cauchy stress vs. Green-Lagrange strain curves of equi-biaxial tensile test of intact aorta and after (a) SDS, and (b) Triton X-100 decellularization. C- circumferential direction; L- longitudinal direction.

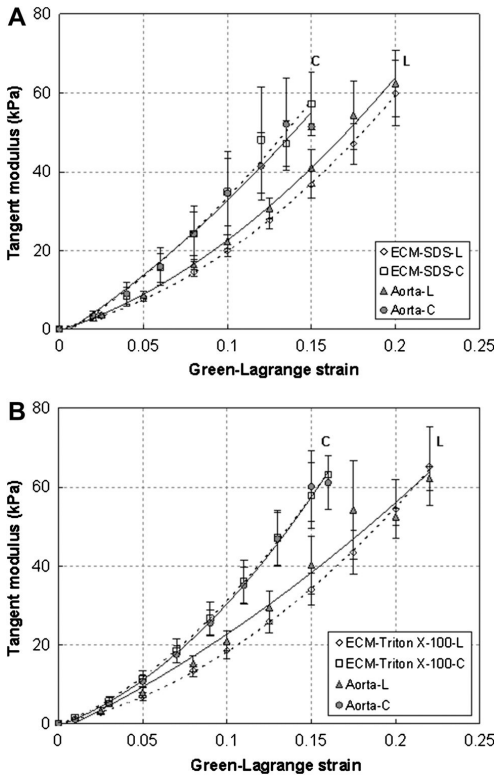

Figure 6.

Averaged tangent modulus in the circumferential (C) and longitudinal direction (L) of the intact aorta and decellularized ECM using (a) SDS (n=9), and (b) Triton X-100 (n=9) treatment. Dashed and solid trend lines are added for decellularized ECM and intact aorta, respectively, to aid viewing.

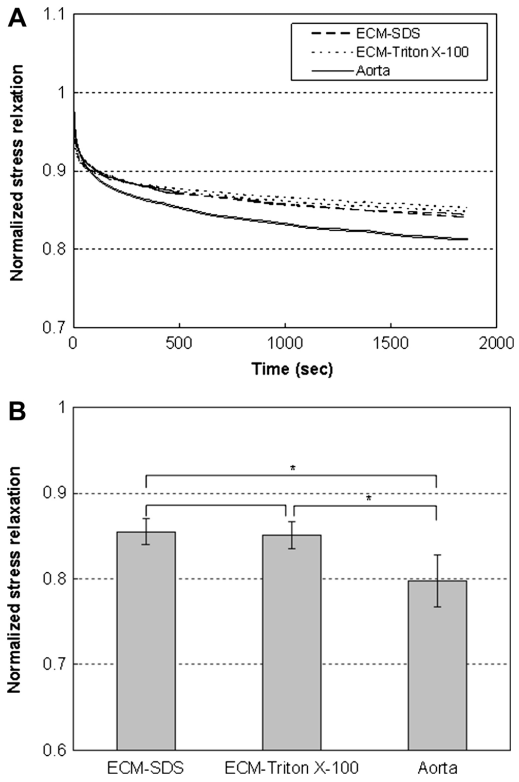

Figure 7.

(a) Representative normalized stress relaxation behavior of SDS and Triton X-100 decellularized ECM and intact aorta samples. Stress relaxation responses in the circumferential and longitudinal directions are almost identical for all samples. (b) Averaged normalized stress relaxation for SDS (n=5), Triton X-100 (n=4) treated ECM and intact aorta (n=4) at initial stress levels of 143.96 ± 8.89 kPa. * indicates the difference is statistically significant ($p < 0.05$).

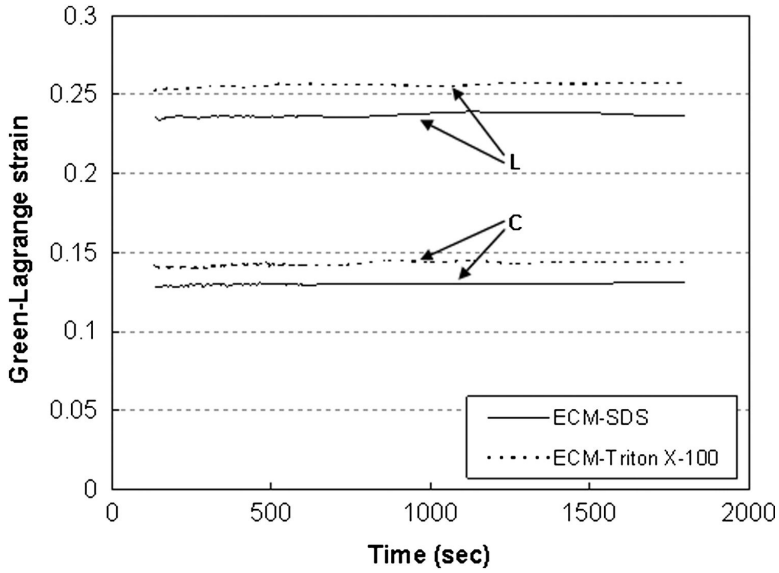

Figure 8.
Representative creep behavior of SDS and Triton X-100 decellularized ECM.